NJC

Accepted Manuscript

Journal Name

Ferrocene-based Polyethyleneimines for Burning Rate Catalysts

Zain-ul-Abdin, Li Wang*, Haojie Yu*, Muhammad Saleem, Muhammad Akram, Nasir M. Abbasi, Hamad Khalid, Ruoli Sun and Yongsheng Chen

Ferrocene-based polymers and derivatives have the ability to catalyze the burning process of composite solid propellants efficiently. However, the simple and volatile ferrocene migrates to the surface of the solid propellant on prolonged storage, which alters the designed burning parameters and causes more seriously unexpected explosions. To retard migration problems, six novel ferrocene-based polyethyleneimines (PEI-Fcs) were synthesized by the condensation reaction of branched polyethyleneimine (PEI) with ferrocenecarbonyl chloride. The structures of the synthesized PEI-Fcs were characterized by ^{1}H NMR, FT-IR and UV-Vis spectroscopy. The redox properties of the polymers are very important for burning rate catalysts (BRCs). The cyclic voltammetry (CV) revealed that all the PEI-Fcs showed redox properties due to the presence of ferrocene moieties. Migration studies confirmed that the migration of these PEI-Fcs was much slower than that of 2,2-bis(ethylferrocenyl)propane (catocene) and ferrocene. The catalytic effect of PEI-Fcs on the thermal decomposition of ammonium perchlorate (AP) was investigated by using thermogravimetry (TG) and differential thermogravimetry (DTG). It was found that in the presence of PEI-Fcs (1–6), the peak decomposition temperature of AP was shifted towards left (decreased) significantly. The results from TG and DTG analysis indicated that novel PEI-Fcs had good catalytic effect on lowering the thermal decomposition temperature of AP and were almost stable up to 220 °C. We expect that these novel PEI-Fcs would have great value as high BRCs for composite solid propellants.

Introduction

Ferrocene-based compounds and derivatives got much attention of the scientists not only from the view point of their reversible redox behavior, high stability and their chemical modification possibilities [1-3], but also due to their increasing applications in many fields such as catalysis, [4-9] nano-materials, [10, 11] medicine, [12] biologically active compounds, [13] material science and ion recognition. [14-16] Ferrocene-based compounds and derivatives are also known as burning rate catalysts (BRCs) for composite solid propellants due to their better microscopic homogeneities in distribution, ignitability of the propellants and good compatibility with organic binder. [17-20] The use of simple ferrocene derivatives as BRCs has inherent drawbacks, such as their migration on storage, evaporation, or sublimation loss during processing and phase separation by crystallization. [21-23] These drawbacks lead to poor aging and irreproducible properties of the propellant [24-26] which reduce service life, change the designed burning parameters and cause more seriously unexpected explosion. [27] The burning rate modifying

effect of ferrocene derivatives fluctuate with chemical structure, solubility, molecular mobility and effective iron content in ferrocene derivatives. [20] Much endeavor was made for the synthesis of ferrocene derivatives with relatively high molecular weight, such as 2,2-bis(ethylferrocenyl)propane (catocene) and *n*-butyl ferrocene [17, 27-32] to overcome these problems and to enhance burning rate of composite solid propellant significantly. However, the study on migration problems is still being continued to find low cost and more efficient way to avoid these problems.

In the field of anti-migration studies, Alper Unever reported migration properties of simple ferrocene derivative (acetyl ferrocene). He found that migration of acetyl ferrocene was observed in significant amount during the curing process even at room temperature, [33] but detailed migration behavior of ferrocene-based hyper-branched polymers in the propellant binder and the difference in the migration behaviors of simple ferrocene and ferrocene-based hyper-branched polymers has not been examined yet. [34]

Ferrocene-based hyper-branched polymers are a new class of functionalized materials, which have attracted considerable attention in the past few years, due to their special three-dimensional structures, high molecular weight, low viscosities and good catalytic and redox properties. [35, 36] Some lateral studies indicated that linking of ferrocenes to the propellant binder via grafting or introducing ferrocenes into the binder

State Key Laboratory of Chemical Engineering, College of Chemical and Biological Engineering, Zhejiang University, Hangzhou 310027, China
Correspondence to Li Wang. E-mail: opl_wl@dial.zju.edu.cn and Haojie Yu. E-mail: hjyu@zju.edu.cn, Tel: +86-571-8795-3200; Fax: +86-571-8795-1612.

ARTICLE

Journal Name

backbone during curing [37-40] or grafting ferrocene on the hyper-branched structures [39] are the effective ways to enhance burning rate and to reduce migration tendency. The Van der Waals forces between ferrocene derivatives (BRCs) and the propellant may be increased by the incorporation of highly electronegative elements (oxygen and nitrogen) into ferrocene-based polymers or their derivatives, which hinder migration of BRCs in composite solid propellant. [20]

Incorporation of ferrocenes into branched structures is a challenge of growing interest for researchers, as it provides a new opportunity to amend unusual properties of the hyper branched polymer. Such ferrocene-based branched polymers have unique and valuable redox properties of ferrocene with low viscosity, high molecular weight and thermal stability. The thermal decomposition of AP is believed to influence propellant combustion behavior, which can be improved by using ferrocene-based polymers or their derivatives that can accelerate the process of low-and high-temperature thermal decomposition.

AP is the most commonly used oxidizer in composite solid propellants due to its excellent burning characteristics, good processability and storability. [36, 41, 42] It has been found that combustion behavior of the propellant is directly affected by the thermal decomposition of AP. [40] The faster AP decomposition results in better performance of the propellant. [43] The thermal decomposition of AP can be accelerated by the

addition of BRCs (ferrocene-based polymers and derivatives) into the propellant. [36]

In this study, to overcome migration problems of BRCs and to enhance burning rate of composite solid propellant, we synthesized six novel PEI-Fcs. The structures of the PEI-Fcs were investigated by nuclear magnetic resonance (^{1}H NMR), Fourier transform infrared (FT-IR) and UV-Vis spectroscopy. As electrochemical properties of the polymers are very important for BRCs to catalyze the burning process of the composite solid propellant due to loss and gain of electrons. So, the electrochemical properties of the synthesized compounds were analyzed by cyclic voltammetry (CV). The thermal behavior and catalytic performance of PEI-Fcs for the thermal decomposition of AP were investigated by TG and DTG techniques and migration behavior of PEI-Fc-1, PEI-Fc-4 and PEI-Fc-6 was also determined.

Results and discussion

Synthesis of PEI-Fcs

Ferrocenecarbonyl chloride was prepared from ferrocenecarboxylic acid by using oxalyl chloride as chlorinating agent in freshly distilled CH_2Cl_2 employing pyridine as a catalyst (Scheme 1).
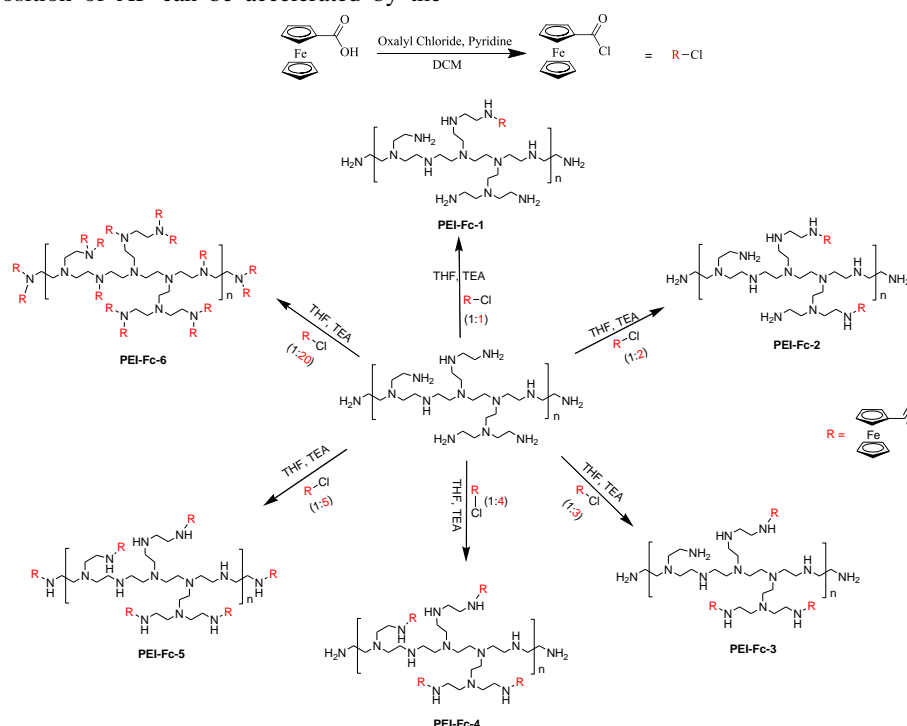
Scheme 1. Syntheses of PEI-Fcs from PEI

PEI-Fcs were prepared by the condensation reaction of ferrocenecarbonyl chloride with PEI, in freshly distilled THF by using TEA as a proton acceptor. The reactions pathways are given in Scheme 1, while the experimental details are given in Table S1.

The structures of PEI-Fcs were elucidated by ^{1}H NMR spectroscopy. On comparison of ^{1}H NMR spectra of PEI-Fcs

with PEI, we found that three new peaks (4.00–5.00 ppm) appeared which were attributed to ferrocenes protons (H-Fc). The intensity of these peaks was increased from PEI-Fc-1 to PEI-Fc-6, while relative intensity of the peaks (0.70-3.80 ppm) attributed to –CH$_2$– protons of PEI (H-PEI) was decreased from PEI-Fc-1 to PEI-Fc-6. The integration ratio of H-Fc (δ ppm: 4.00-5.00) with H-PEI (0.70-3.80 ppm) was according to the

required ratio of the structures, which indicated that PEI-Fcs were synthesized successfully. The ^{1}H NMR spectra of PEI-Fc-1 with following chemical shifts (δ in ppm): 4.00-5.00 (H-Fc) and 0.70-3.80 (H-PEI) with integration ratio (1:4.36), PEI-Fc-2 with chemical shifts: 4.00-5.00 (H-Fc) and 0.70-3.80 (H-PEI) with integration ratio (1:2.42), PEI-Fc-3 with chemical shifts: 4.00-5.00 (H-Fc) and 0.70-3.80 (H-PEI) with integration ratio (1:1.51), PEI-Fc-4 with chemical shifts: 4.00-5.00 (H-Fc) and 0.70-3.80 (H-PEI) with integration ratio (1:1.25), PEI-Fc-5 with chemical shifts: 4.00-5.00 (H-Fc) and 0.70-3.80 (H-PEI) with integration ratio (1:1.20) and PEI-Fc-6 with chemical shifts: 4.00-5.00 (H-Fc) and 0.70-3.80 (H-PEI) with integration ratio (1:0.45) were obtained. The ^{1}H NMR spectra of PEI and PEI-Fcs are shown in Figure S1.

The structures of PEI-Fcs were further confirmed by the FT-IR spectra. The intensity of the stretching vibrations of N–H of amino groups at 3500-3300 cm^{-1} was decreased from PEI-Fc-1 to PEI-Fc-5 and disappeared in the FT-IR spectrum of PEI-Fc-6. The intensity of the stretching and bending vibrations of N-H of amides at 3,100 cm^{-1} and 1,550 cm^{-1}, respectively was increased from PEI-Fc-1 to PEI-Fc-5 and no such vibrations were observed in the FT-IR spectra of PEI and PEI-Fc-6. Meanwhile, a new peak at 1,690–1,700 cm^{-1} assigned to C=O stretching vibrations of amides and vibrational and deformational bands of ferrocenyl rings at 1,023–1,045, 801–820 and 496–502 cm^{-1} were also observed in FT-IR spectra of PEI-Fcs. [34] FT-IR spectra of PEI and PEI-Fcs are shown in Figure 1. These FT-IR results support the synthesis of PEI-Fcs.
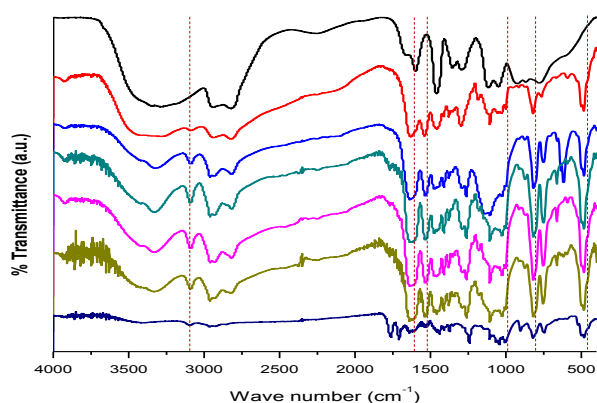

Figure 1. FT-IR spectra of: (a) PEI, (b) PEI-Fc-1, (c) PEI-Fc-2, (d) PEI-Fc-3, (e) PEI-Fc-4, (f) PEI-Fc-5 and (g) PEI-Fc-6.

The UV–Vis absorption spectra of PEI-Fcs (**1-6**) (Figure S2) (c = 0.05 mM) in dichloromethane showed the absorption bands with λ_{max} around 265 nm and 235 nm which can be assigned to π-π* transitions, while absorption bands with λ_{max} around 310 nm and 445 nm can be assigned to the charge transfer band (CT) and d-d transitions, respectively. [19] In all PEI-Fcs, intense absorption bands corresponding to π-π* transitions were observed. In case of PEI-Fc-6, more intense absorption bands corresponding to d-d transitions and CT were observed, while in case of PEI-Fc-1, PEI-Fc-2 and PEI-Fc-3, no absorption bands corresponding to d-d transitions and CT were observed. As ferrocene moieties in PEI-Fcs were increased, CT absorption band become more intense.

Electrochemical behavior of PEI-Fcs

The electrochemical properties of polymers are very important to investigate potential application as BRCs. The redox polymer has well-defined redox properties. [44] Furthermore, CV is considered as one of the most effective methods to study the electrochemical properties of the polymers. [45] The PEI-Fcs have good solubility in many solvents with different polarities. So, the electrochemical behavior of PEI-Fcs (0.5 mmol L^{-1}) was studied in DCM, THF, CHCl$_3$, DMF and DMSO containing Bu$_4$NBF$_4$ (0.10 M) as a supporting electrolyte at 20 °C. The CV results indicated that polarity of the solvent and potential scan rate have great effect on the CV behavior of PEI-Fcs. [46-50]

The organic solvents affected the shape of the CV curves due to the change in the polarity. The increase in the polarity of the solvent led to deformation of the peak shapes. For all PEI-Fcs, the shape of the CV curve was deformed in DMF and DMSO, while in case of PEI-Fc-1, shape was also deformed in THF and peak current was decreased, while reduction peak potential was increased with the increase of the solvent polarity, which indicated that solvent polarity was inversely proportional to the reduction of PEI-Fcs. [51] In case of DMSO, an abnormal behavior was observed, which might be due to the interaction of PEI-Fcs with DMSO and high viscosity of DMSO. Some of physical parameters of the solvents used are listed in Table S2. [52, 53]

The most well-defined and sharp peaks were obtained in DCM, CHCl$_3$ and THF with the highest current in DCM. The highest peak-to-peak potential separation (ΔE_p) was obtained in CHCl$_3$ and the lowest ΔE_p values were obtained in DCM. This data indicates that the rate of the electrode reaction was decreased from DCM to CHCl$_3$. Thus, the resistance of the solution was smaller and the diffusion rate of the charge was faster in DCM than CHCl$_3$, which indicates that the redox reaction occurs easily in DCM as compared to CHCl$_3$. Electrochemical data of PEI-Fc-1 to PEI-Fc-5, in different organic solvents at 0.1 V/s scan rate is shown in Table S4, while in case of PEI-Fc-6, no clear redox peaks were observed for the analysis of electrochemical data.

The electrochemical behavior of PEI-Fcs was studied at different potential scan rates in DCM, CHCl$_3$, THF, DMF and DMSO, respectively. The typical CV curves of PEI-Fc-1 to PEI-Fc-6 at different potential scan rates (ν) of 0.1, 0.2, 0.3, 0.4 and 0.5 V/s are shown in Figures S3-S8, respectively, while the electrochemical data is shown in Tables S5-S9.

It was found that the shape of the CV curves of PEI-Fcs was sensitive to the scan rate. Additionally, the peak current values of PEI-Fcs solutions, i_{pa} and i_{pc}, were increased with the increase in scan rate. Furthermore, the rate of increase in the reduction peak current (i_{pc}) was higher than the rate of increase in the oxidation peak current (i_{pa}). According to the electrochemical theory, [54] these results indicate that at room temperature, the charge transport of the electrode processes obeyed Fick's law and also the electrode processes were diffusion control over the detected scan rate range for PEI-Fcs.

Migration Studies

PEI-Fc-1, PEI-Fc-4 and PEI-Fc-6 were analyzed for migration studies in comparison with those of catocene and ferrocene (detail is given in Table S11). It was observed that migration of PEI-Fc-1, PEI-Fc-4 and PEI-Fc-6 was much slower than catocene and ferrocene. The synthesized PEI-Fcs have high molecular weight, highly branched structure and large number of N-H groups. Due to the presence of large number of N-H groups, Van der Waals forces were developed between PEI-Fcs and propellant. The strong Van der Waals forces and low vapour pressure (due to high molecular weight) of PEI-Fcs were resulted in lower migration of PEI-Fcs.

PEI shows least migration due to highly branched structure, high molecular weight and formation of strong Van der Waals forces between PEI and propellant. So, we modified PEI to PEI-Fcs, to enhance burning rate catalytic activity and to reduce migration problems. It was observed that migration tendency was increased with the increase in ferrocene moieties in PEI-Fcs. Possibly, as relatively less number of ferrocene moieties was present in PEI-Fc-1, so relatively lowest migration was observed in PEI-Fc-1. Among PEI-Fcs, maximum migration was observed in PEI-Fc-6 due to the presence of relatively large number of ferrocene moieties.
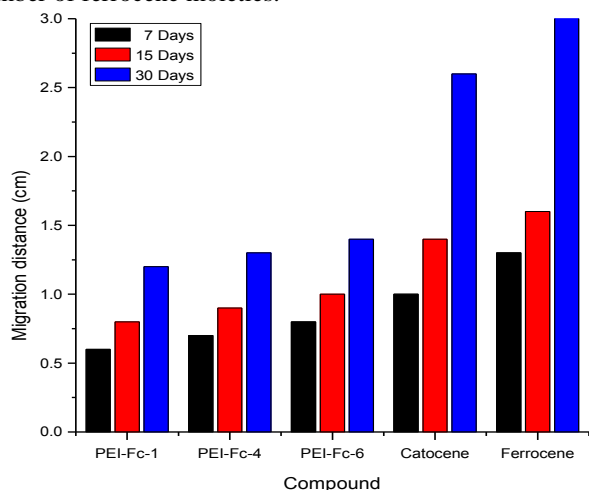

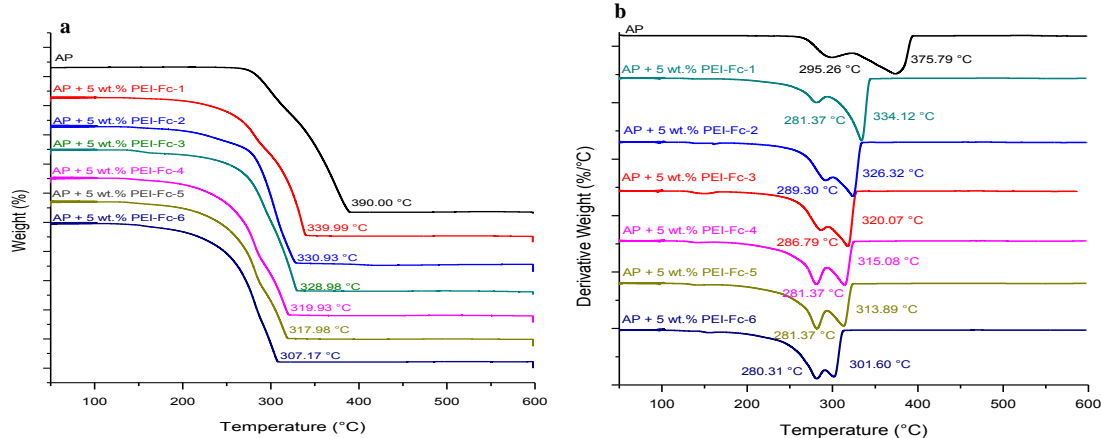**Figure 2.** Migration studies of PEI-Fc-1, PEI-Fc-4, PEI-Fc-6, catocene and ferrocene at 50 °C.

The migration study of the PEI-Fc1, PEI-Fc-4 and PEI-Fc-6 in comparison with ferrocene and catocene is shown in Figure 2 and migration photos are shown in Figure S9. The size of the tubes used for migration studies was around 7 cm. The migration mechanism of PEI-Fc-6 from inner part to the interface of the propellant is shown in Figure 3.

Catalytic performances for the thermal decomposition of AP

Thermal stability is an extremely important parameter for BRCs. All the newly synthesized PEI-Fcs were stable up to 220 °C. The catalyst having high thermal stability will be beneficial to its catalytic activity and for the combustion process of the solid composite propellant.
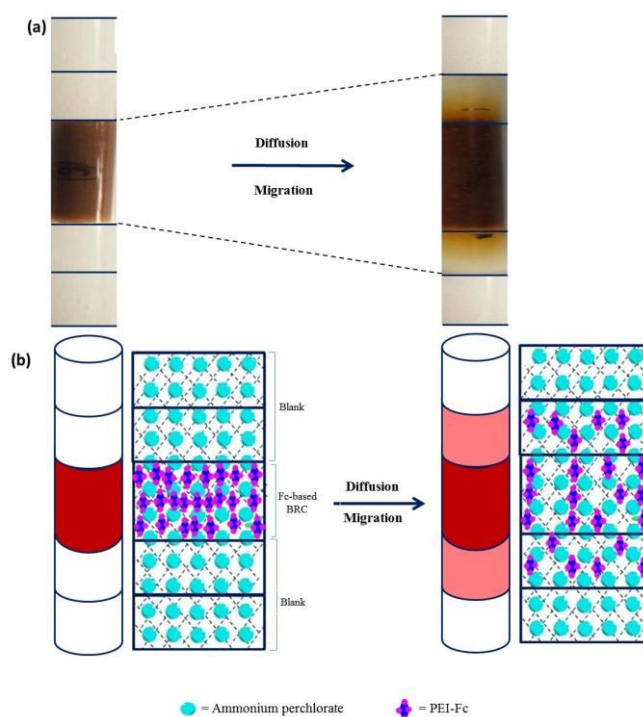

Figure 3. Migration mechanism of PEI-Fc-6 from inner part to the interface of the propellant: (a) Sample (PEI-Fc-6), (b) Model of the sample.

Figure 4. (a) TG curves of pure AP and 5 wt. % PEI-Fcs and (b) DTG curves of pure AP and 5 wt. % of PEI-Fcs
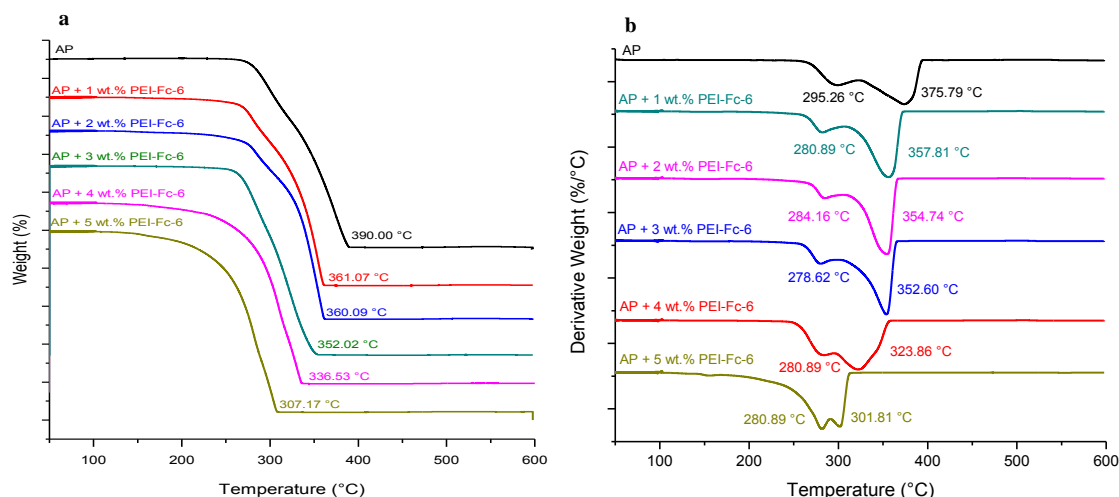
Journal Name

ARTICLE

Figure 5. (a) TG curves of pure AP and AP with different wt. % (1-5) PEI-Fc-6 and (b) DTG curves of pure AP and AP with different wt. % (1-5) PEI-Fc-6

AP is a commonly used main component in hydroxyl terminated polybutadiene-ammonium perchlorate (HTPB–AP) composite solid propellants. Its thermal decomposition has a close relationship with the combustion process of the solid propellant. Therefore, the catalytic performance of the BRCs on the combustion behavior of HTPB–AP solid propellant is usually assessed by its effect on the thermal decomposition temperature of AP. The addition of a ferrocene-based BRCs as additive gives rise a shift (towards left) in the peak temperature of AP and accelerates AP decomposition as well as increases the amount of heat released by thermal decomposition of AP.[55]

The catalytic performances of all the synthesized PEI-Fcs on thermal decomposition of AP were evaluated by TG/DTG techniques. The catalytic effect of PEI-Fcs was evaluated by using 5% of PEI-Fcs on the decomposition of AP (Figure 4). The detail for the samples preparation is given in Table S12. The catalytic effect of PEI-Fc-6 on the thermal decomposition of AP was also evaluated by varying the contents (1-5 wt. %) of PEI-Fc-6 (Figure 5). It was observed that in case of pure AP, decomposition occurred at 390.00 °C, but by the addition of 5 wt. % of PEI-Fcs and different wt. % (1-5) of PEI-Fc-6, decomposition peaks were shifted toward left. The burning rate catalytic activity of BRCs is assessed by the thermal decomposition of AP. As Fc moieties in PEI-Fcs were increased, decomposition temperature of AP was significantly decreased.
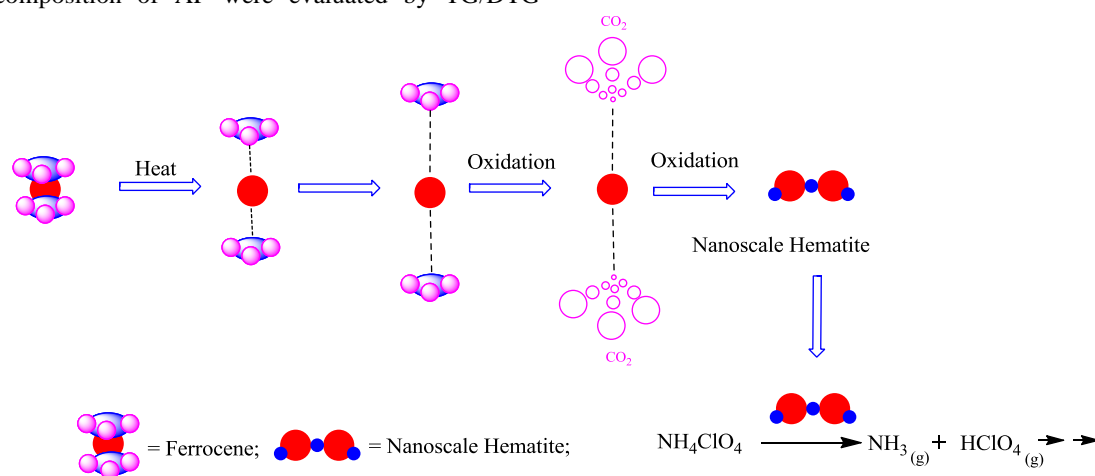

Figure 6. The possible mechanism for the decomposition of AP catalyzed by ferrocene-based burning rate catalyst.

Journal Name

ARTICLE

Due to the presence of relatively large number of ferrocene moieties in PEI-Fc-6, it showed maximum lower shift in the thermal decomposition temperature of AP, which was observed at 307.17 °C for 5 wt. % PEI-Fc-6 (Figure 4a). Similarly, as wt. % of PEI-Fc-6 was increased, the decomposition temperature was decreased (Figure 5a). Among PEI-Fcs, PEI-Fc-6 showed best catalytic activity on the thermal decomposition temperature of AP. DTG curves showed that pure AP and all the PEI-Fcs were decomposed in two stages. First stage decomposition corresponding to low temperature decomposition (LTD), while second stage decomposition corresponding to high temperature decomposition (HTD). In case of pure AP, LTD was observed at 297.10 °C and HTD was observed at 376.69 °C, while in case of PEI-Fcs, LTD was observed around 280 °C and HTD was observed around 320 °C. In case of PEI-Fcs, as ferrocene moieties were increased, weight loss at first stage was increased. The maximum weight loss at first stage was observed for 5 wt. % PEI-Fc-6 (Figure 4b). Similarly, as wt. % of PEI-Fc-6 was increased, first stage decomposition was increased (Figure 5b).

Both the LTD and HTD stages of the AP were significantly affected by the addition of PEI-Fcs. These results show that these newly synthesized PEI-Fcs have good catalytic effect on lowering the thermal decomposition temperature of AP.

Possible burning rate catalytic mechanism of ferrocene-based compounds on the thermal decomposition of AP

In the combustion of solid composite propellant containing AP, thermal decomposition of AP is considered as first step. [56] As AP contains four different elements like nitrogen, hydrogen, chlorine and oxygen, so its decomposition is little bit complicated. By considering oxidation potential of these elements, many possible mechanisms (like proton-transfer, electron-transfer, forming transition-metal materials, acid-base interaction mechanism, etc.) have been proposed. Fc-based polymers and derivatives have high redox potential (E_{red}) and their E_{red} value depends upon the nature of the substituent on the ferrocene ring. [20, 57] On combustion of solid propellant containing Fc-based BRCs, iron atom of ferrocene moiety changes into iron oxides. When ferrocene-based polymers and derivatives are heated, at the start, the distance between Cp rings and iron atom increases and then ferrocene unit begins to decompose, which results in the oxidation of Cp rings of ferrocene to produce CO_2. In the same time, iron atom of ferrocene moiety reacts with oxygen to form nanoscale hematite. The nanoscale hematite particles possess larger surface area in comparison with powdered hematite and show excellent burning rate catalytic activity on the decomposition of AP. These nanoscale particles accelerate the decomposition of AP by proton transfer (N-H bond cleavage) from NH_4ClO_4 to NH_3 and $HClO_4$, which further involve redox process to produce gaseous products. PEI contributes in the reduction of migration problems on prolong storage due to its high molecular weight, highly branched structure and formation of strong Van der Waals forces between PEI-Fcs and propellant due to the presence of large number of N-H groups in PEI. On heating, AP generates oxygen which is used for the oxidation of iron atom of ferrocene to nanoscale hematite. These produced nanoscale hematite catalyze the decomposition of AP. The decomposition of AP is considered as rate determining step. The burn rate equation used for determining burning rate is given in equation 1. [58]

$$\text{Burn rate (r)} = r° + \ b\ P^a \longrightarrow \quad (1)$$

Whereas "r" is the burn rate, "r°" is a constant (usually taken as zero), "b" is a burn rate coefficient (constant due to the material) and "a" is the pressure exponent. To avoid unstable combustion, burn rate or catalysis can be achieved while pressure exponent falls. As burn rate increases with the increase in pressure but after specific increase in pressure, no increase in burn rate occurs and unstable combustion occurs. To avoid unstable combustion, the value of the pressure exponent should be 0.3 to 0.6. Due to the non-linearity of the pressure-burn rate relationship, it is necessary to reduce pressure significantly to get desired burning rate. [58] The possible mechanism for the decomposition of AP catalyzed by Fc-based BRCs is shown in Figure 6.

LTD of AP continues through dissociative sublimation followed by multiphase reactions, which leads to porous AP. [59] The reactions of the gaseous products compete with dissociative sublimation during HTD. [60] The preference of one process on the other depends on the reaction conditions. Confined conditions favor gas phase reactions to proceed in the condensed phase.

Conclusion

In this paper, six new ferrocene-based polyethyleneimines (PEI-Fcs) have been synthesized successfully in view of their potential to lower migration in comparison with catocene and to enhance burning rate of composite solid propellant. All the synthesized PEI-Fcs were thermally stable and low-migratory. UV–Vis absorption spectra indicated that PEI-Fc-4, PEI-Fc-5 and PEI-Fc-6 showed photo-induced charge transfer effect and it was more prominent in PEI-Fc-6. The electrochemical investigations showed that the two reversible oxidation waves were controlled by diffusion. TG and DTG results confirmed

that these PEI-Fcs have high catalytic activity on lowering thermal decomposition temperature of ammonium perchlorate (AP) and PEI-Fc-6 lowers the thermal decomposition temperature of AP more dramatically up to 307.17 °C. On the basis of these results, we can say that these low-migratory novel PEI-Fcs have potential effect on lowering thermal decomposition temperature of AP.

Experimental

Materials

Polyethyleneimine, branched (Mn = 10,000) (PEI) was purchased from Sigma Aldrich and was used without further purification. Dichloromethane (DCM), tetrahydrofuran (THF), and triethylamine (TEA) were purchased from Sinopharm Chemical Reagent Co., Ltd. and were used after drying by using 4A-type molecular sieves followed by reflux system. Pyridine, chloroform, and petroleum ether were purchased from Sinopharm Chemical Reagent Co., Ltd. and were used after drying by using 4A-type molecular sieves. Oxalyl chloride, ferrocenecarboxylic acid and $NaHCO_3$ were purchased from Sinopharm Chemical Reagent Co., Ltd. and were used without further purification.

Synthesis

Ferrocenecarbonyl chloride

Ferrocenecarbonyl chloride was prepared from ferrocenecarboxylic acid by using oxalyl chloride as chlorinating agent in freshly distilled dichloromethane employing pyridine as a catalyst. In typical procedure, ferrocenecarboxylic acid (10.36 g, 41.96 mmol) was dried under vacuum at 40 °C for 4 h. The dried ferrocenecarboxylic acid was dissolved in 75 mL freshly distilled dichloromethane and resulting solution was stirred well under Ar atmosphere at 25 °C. Pyridine (7.25 mL) was added to the previous solution. Oxalyl chloride (7.75 mL, 90.36 mmol) was also added drop wise to the previous solution at 25 °C. The reaction mixture was stirred for 30 min at room temperature (25 °C), and then refluxed for 6 h. The contents of the reaction flask were evaporated to dryness under reduced pressure and the residue was extracted with petroleum ether at 90 °C.

PEI-Fc-1 to PEI-Fc-5

As synthetic procedure for PEI-Fc-1 to PEI-Fc-5 was same. So, synthesis of PEI-Fc-1 was taken as an example. PEI-Fc-1 was prepared by the condensation reaction of ferrocenecarbonyl chloride with polyethyleneimine, branched (PEI). In typical procedure, PEI was dried under vacuum and then dissolved in freshly distilled THF. TEA was added to the PEI solution. Afterward, a solution of ferrocenecarbonyl chloride in freshly distilled THF was added drop wise to the previous solution. The solution was then stirred for 18 h at 25 °C. Solvent was evaporated on rotary evaporator. The residue was dissolved in $CHCl_3$ and washed (four times) with 1% $NaHCO_3$ solution in

distilled water followed by washing (three times) with distilled water. The organic layer was separated, anhydrous Na_2SO_4 was added and putted overnight. The mixture was filtered to separate Na_2SO_4 and resulting filtrate was dried on rotatory evaporator to get product. The product was further dried in vacuum oven at 45 °C for 2 days. Experimental details are given in Table S1.

PEI-Fc-6

PEI-Fc-6 was synthesized by the condensation reaction of ferrocenecarbonyl chloride with PEI. The PEI was dried under vacuum and then dissolved in freshly distilled THF. TEA was added to the PEI solution. Afterward, a solution of ferrocenecarbonyl chloride in freshly distilled THF was added drop wise to the previous solution. The solution was then stirred for 20 h at 25 °C followed by the refluxed for 5 h. Solvent was evaporated on rotary evaporator. The residue was dissolved in $CHCl_3$ and washed (four times) with 1% $NaHCO_3$ solution in distilled water followed by washing (three times) with distilled water. The organic layer was separated, anhydrous Na_2SO_4 was added and putted overnight. The mixture was filtered to separate Na_2SO_4, and resulting filtrate was dried on rotatory evaporator to get product. The product was further dried in vacuum oven at 45 °C for 2 days. Experimental details are given in Table S1.

Characterization

Spectroscopy

^{1}H NMR spectra were recorded on a 500 MHz AVANCE NMR spectrometer (Model DMX-400). The chemical shifts were related to tetramethylsilane (TMS) at δ = 0 ppm by using $CDCl_3$ as a solvent.

FT-IR spectra were recorded on a Nicolet 5700 infrared spectrometer. The synthesis of PEI-Fcs were also verified by FT-IR. FT-IR spectra of the synthesized PEI-Fcs were reordered by KBr pellet technique. 4% sample and KBr were crushed to a powder, mixed together and KBr pellet was prepared, while FT-IR spectrum of PEI was recorded by using KBr glass. PEI was putted on KBr glass and film was prepared.

UV-Vis spectra were reordered on 3802 UV-Vis unico spectrophotometer. Samples solutions (c=0.05 mM) were prepared by dissolving 0.00125 mmol of PEI-Fcs in 25 mL DCM at 20 °C (detail is given in Table S3).

Cyclic voltammetry

The CV was carried out on a CHI-630A electrochemical analyzer (CH Instruments, Inc., Austin, Texas) in an undivided three-electrode cell. All electrodes were from CH instruments. The working electrode was a Teflon-shrouded platinum disk electrode with a diameter of 2 mm for the solution test. The working electrode was polished to a mirror finish with 0.05 µm Al_2O_3 paste on felt, cleaned by ultra-sonication successively in 0.1 M NaOH, 1:1 HNO_3, anhydrous ethyl alcohol, doubly distilled water, then dried and used for the electrochemical measurements. A platinum wire electrode was used as the

counter electrode. The reference electrode was an Ag wire electrode for solution test. CV solutions were prepared by dissolving 0.005 mmol of PEI-Fcs and 1.00 mmol of Bu_4NBF_4 in 10 mL solvent (DCM, THF, $CHCl_3$, DMF, and DMSO, respectively) at 20 °C (detail is given in Table S10).

Thermal analysis

TG and DTG analysis were performed on a Perkin-Elmer Pyris 1 thermogravimetric instrument at a heating rate of 5 °C/min under nitrogen in the range of 50-600 °C. To investigate catalytic performance of the synthesized PEI-Fcs on thermal decomposition of AP, specific amount of PEI-Fcs and AP were mixed and grinded in a certain weight ratio for TG and DTG analysis. The detail for the sample preparation is given in Table S12.

Sample preparation for migration studies

The samples of PEI-Fcs used for migration studies were consisted of three adjacent parts; unloaded part (blank), interface and loaded part. These three components correspond to insulation, liner and propellant, respectively. The unloaded part was consisted of AP, hydroxyterminated polybutadiene (HTPB) and isophorone diisocyanate (IPDI) and was prepared by mixing AP, HTPB and IPDI (at wt. % of 71.93, 21.28 and 6.79, respectively) for 30 min to obtained homogeneous slurry. The ratio of the NCO groups in IPDI to the –OH groups was according to hydroxyl value of HTPB. The resulting mixture was cast into molds and cured at room temperature (25 °C) for 3 days before undergoing accelerated aging.

The loaded part was consisted of AP, HTPB, IPDI and a burning rate catalyst (PEI-Fcs) and was prepared by mixing AP, HTPB, IPDI and PEI-Fcs (PEI-Fc-1, PEI-Fc-4 and PEI-Fc-6 at wt. % of 70.6, 20.1, 6.2 and 3.0, respectively) were blended for approximately 1 h. The resulting mixture was subsequently cast on an unloaded layer that had been cured for 3 days. After curing for 3 days at room temperature, all the prepared samples were aged in an oven at 50 °C for 30 days. The detail is given in Table S11.

Acknowledgments

References

1. H. D. Li, Z. H. Ma, K. Yang, L. L. Xie and Y. F. Yuan, *J. Mol. Struct.*, 2012, **1024**, 40-46.
2. B. Wei, Y. Gao, C. X. Lin, H. D. Li, L. L. Xie and Y. F. Yuan, *J. Organomet. Chem.*, 2011, **696**, 1574-1578.
3. M. Saleem, H. Yu, L. Wang, A. Zain ul, H. Khalid, M. Akram, N. M. Abbasi and J. Huang, *Anal. Chim. Acta*, 2015, **876**, 9-25.
4. M. Drusan and R. Sebesta, *Tetrahedron*, 2014, **70**, 759-786.
5. D. J. Young, S. W. Chien and T. S. A. Hor, *Dalton Trans.*, 2012, **41**, 12655-12665.
6. D. Schaarschmidt and H. Lang, *Organometallics.*, 2013, **32**, 5668-5704.
7. V. H. Purecha, N. S. Nandurkar, B. M. Bhanage and J. M. Nagarkar, *Tetrahedron Lett.*, 2008, **49**, 5252-5254.
8. Z. Cheng, G. Zhang, X. Fan, F. Bi, F. Zhao, W. Zhang and Z. Gao, *Inorg. Chim. Acta*, 2014, **421**, 191-199.
9. R. Kurane, V. Gaikwad, J. Jadhav, R. Salunkhe and G. Rashinkar, *Tetrahedron Lett.*, 2012, **53**, 6361-6366.
10. A. W. Orbaek, N. Aggarwal and A. R. Barron, *J. Mate. Chem. A*, 2013, **1**, 14122-14132.
11. G. Huang and J. Weng, *Curr. Org. Chem.*, 2011, **15**, 3653-3666.
12. S. S. Braga and A. M. S. Silva, *Organometallics.*, 2013, **32**, 5626-5639.
13. P. Z. Li and Z. Q. Liu, *Eur. J. Med. Chem.*, 2011, **46**, 1821-1826.
14. P. Molina, A. Tarraga and M. Alfonso, *Dalton Trans.*, 2014, **43**, 18-29.
15. M. Alfonso, A. Espinosa, A. Tarraga and P. Molina, *Chem. Commun*, 2012, **48**, 6848-6850.
16. S. R. Beeren and J. K. M. Sanders, *JACS*, 2011, **133**, 3804-3807.
17. J. m. Gao, L. Wang, H. j. Yu, A. g. Xiao and W. b. Ding, *Propell. Explos. Pyrot.*, 2011, **36**, 404-409.
18. N. Dilsiz and A. Unver, *J. Appl. Polym. Sci.*, 2006, **101**, 2538-2545.
19. Z. M. Lai, H. M. Ye, Q. Wan, L. L. Xie, S. Bai and Y. F. Yuan, *J. Mol. Struct.*, 2014, **1059**, 33-39.
20. A. Zain ul, H. Yu, L. Wang, M. Saleem, H. Khalid, N. M. Abbasi and M. Akram, *Appl. Organomet. Chem.*, 2014, **28**, 567-575.
21. P. J. Swarts, M. Immelman, G. J. Lamprecht, S. E. Greyling and J. C. Swarts, *S. Afr. J. Chem.*, 1997, **50**, 208-216.
22. H. Yu, L. Wang, J. Huo, J. Ding and Q. Tan, *J. Appl. Polym. Sci.*, 2008, **110**, 1594-1599.
23. F. Xiao, F. Feng, L. Li and D. Zhang, *Propell. Explos. Pyrot.*, 2013, **38**, 358-365.
24. K. F. Grythe and F. K. Hansen, *J. Appl. Polym. Sci.*, 2007, **103**, 1529-1538.
25. L. Gottlieb and S. Bar, *Propell. Explos. Pyrot.*, 2003, **28**, 12-17.
26. F. Xiao, X. Yu, F. Feng, X. Sun, X. Wu and Y. Luo, *J. Inorg. Organomet. Polym. Mater.*, 2012, **23**, 315-324.
27. X. Liu, W. Zhang, G. Zhang and Z. Gao, *New J. Chem.*, 2015, **39**, 155-162.
28. K. Menke, P. Gerber, E. Geissler, G. Bunte, H. Kentgens and R. Schoffl, *Propell. Explos. Pyrot.*, 1999, **24**, 126-133.
29. G. M. Gore, K. R. Tipare, R. G. Bhatewara, U. S. Prasad, M. Gupta and S. R. Mane, *D. Sci. J.*, 1999, **49**, 151-158.
30. R. Tong, Y. Zhao, L. Wang, H. Yu, F. Ren, M. Saleem and W. A. Amer, *J. Organomet. Chem.*, 2014, **755**, 16-32.

31. X. Zhang, Y. Xia, L. Jia, J. Chi, W. Chang and J. Wang, *Huaxue Tuijinji Yu Gaofenzi Cailiao*, 2012, **10**, 58-64.

32. X. Liu, D. Zhao, F. Bi, X. Fan, F. Zhao, G. Zhang, W. Zhang and Z. Gao, *J. Organomet. Chem.*, 2014, **762**, 1-8.

33. A. Ünver, N. Dilsiz, M. Volkan and G. Akovalı, *J. Appl. Polym. Sci.*, 2005, **96**, 1654-1661.

34. F. Xiao, M. Shi, P. Lei, Y. Luo and J. Zhao, *J. Inorg. Organomet. Polym. Mater.*, 2011, **21**, 175-181.

35. H. Dong, A. Qin, C. K. W. Jim, J. W. Y. Lam, M. Haeussler and B. Z. Tang, *J. Inorg. Organomet. Polym. Mater.*, 2008, **18**, 201-205.

36. R. Sun, L. Wang, H. Yu, A. Zain ul, Y. Chen, H. Khalid, N. Abbasi and M. Akram, *J. Inorg. Organomet. Polym. Mater.*, 2014, **24**, 1063-1069.

37. K. Subramanian, *J. Polym. Sci., Part A: Polym. Chem.*, 1999, **37**, 4090-4099.

38. B. S. Cho and S. T. Noh, *J. Appl. Polym. Sci.*, 2011, **121**, 3560-3568.

39. F. Xiao, F. Feng, L. Li and D. Zhang, *Propell. Explos, Pyrot.*, 2013, **38**, 358-365.

40. F. Xiao, X. Sun, X. Wu, J. Zhao and Y. Luo, *J. Organomet. Chem.*, 2012, **713**, 96-103.

41. M. Kohga and K. Okamoto, *Combust. Flame*, 2011, **158**, 573-582.

42. J. K. Sharma, P. Srivastava, G. Singh, M. S. Akhtar and S. Ameen, *Ceram. Int.*, 2015, **41**, 1573-1578.

43. H. Zhao, M. Chen, X. Zhu, S. Chen and Z. Bian, *Res. Chem. Intermed.*, 2013, DOI: 10.1007/s11164-013-1503-7, Ahead of Print.

44. J. L. DeLuca, D. P. Hickey, D. A. Bamper, D. T. Glatzhofer, M. B. Johnson and D. W. Schmidtke, *Chem. Phys. Chem.*, 2013, **14**, 2149-2158.

45. N. G. Tsierkezos, *J. Solution. Chem.*, 2007, **36**, 289-302.

46. L. Ma, L. Wang, Q. Tan, H. Yu, J. Huo, Z. Ma, H. Hu and Z. Chen, *Electrochim. Acta*, 2009, **54**, 5413-5420.

47. Q. Tan, L. Wang, L. Ma, H. Yu, Q. Liu and A. Xiao, *Macromolecules.*, 2009, **42**, 4500-4510.

48. C. Li, L. Wang, L. Deng, H. Yu, J. Huo, L. Ma and J. Wang, *J. Phys. Chem. B*, 2009, **113**, 15141-15144.

49. Q. Tan, L. Wang, L. Ma, H. Yu, J. Ding, Q. Liu, A. Xiao and G. Ren, *J. Phys. Chem. B*, 2008, **112**, 11171-11176.

50. H. Yu, L. Wang, J. Huo, C. Li and Q. Tan, *Des. Monomers. Polym.*, 2009, **12**, 305-313.

51. T. Chen, L. Wang, G. Jiang, J. Wang, X. j. Wang, J. Zhou, J. Wang, C. Chen, W. Wang and H. Gao, *J. Electroanal. Chem.*, 2006, **586**, 122-127.

52. W. Linert, Y. Fukuda and A. Comard, *Coordin. Chem. Rev.*, 2001, **218**, 113-152.

53. I. M. Smallwood, *John Wiley & Sons, New York*, 1996.

54. A. Bard and L. Faulkner, *Electrochemical methods fundamentals and applications*, John Wiley & Sons, *New York*, 2001.

55. Q. Yang, S. Chen, G. Xie and S. Gao, *J. Hazard. Mater.*, 2011, **197**, 199-203.

56. K. Fujimura and A. Miyake, *J. Therm. Anal. Calorim.*, 2010, **99**, 27-31.

57. M. Suhithi, G. I. Peiris and T. P. Pongilinan, *J. Phys. Chem. A*, 2000, **104**, 11188-11193.

58. A. I. Atwood, K. P. Ford and C. J. Wheeler, *Prog. Propul. Phys.,* 2013, **4**, 3-14.

59. V. V. Boldyrev, *Thermochim. Acta*, 2006, **443**, 1-36.

60. S. Vyazovkin and C. A. Wight, *Chem. Mater.*, 1999, **11**, 3386-3393.
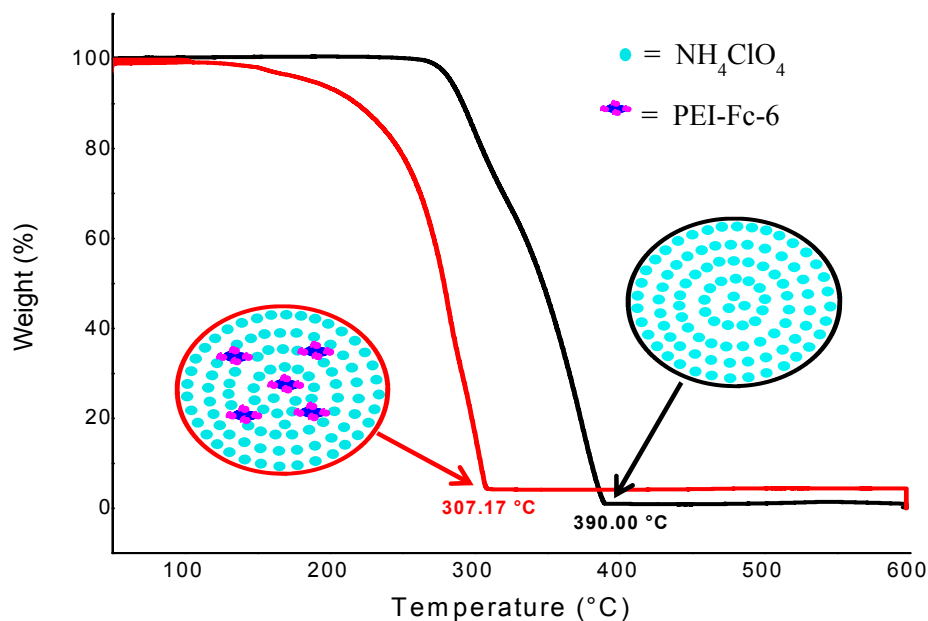
Ferrocene-based Polyethyleneimines for Burning Rate Catalysts

Zain-ul-Abdin, Li Wang[*], Haojie Yu[*], Muhammad Saleem, Muhammad Akram, Nasir M.

Abbasi, Hamad Khalid, Ruoli Sun and Yongsheng Chen

State Key Laboratory of Chemical Engineering, College of Chemical and Biological Engineering,

Zhejiang University, Hangzhou 310027, China

GRAPHIC

Text

Synthesis, electrochemical behavior, burning rate catalytic performance, burning rate catalytic

and migration mechanism of ferrocene-based polyethyleneimines.

[*] Correspondence to Li Wang. E-mail: opl_wl@dial.zju.edu.cn and Haojie Yu. E-mail: hjyu@zju.edu.cn
Tel: +86-571-8795-3200; Fax: +86-571-8795-1612.